GUIDE-CHAIN CONTACT PRESSURE TRIBOLOGICAL ANALYSIS

Radu PAPUC[1], Radu VELICU[2], Mihai – Tiberiu LATES[3]

[1] Transilvania University of Brasov, radu.papuc@unitbv.ro
[2] Transilvania University of Brasov, rvelicu@unitbv.ro
[3] Transilvania University of Brasov, latesmt@unitbv.ro

Abstract—The paper presents the analysis of tribological contacts between the tensioning guide and toothed chain generally used in the combustion engines. First it is identified geometry which define the contact between the tensioning guide and the toothed chain. To determine the pressure distribution in the contact area between tensioning guide and links, is necessary to resolve the Reynolds equation. So, a general methodology is proposed for contacts of this type. Then, the mathematical modeling and numerical solution obtained are presented for a specific optimization problem of the tensioning guide and link contact.

Keywords— chain, pressure, tensioning guide, Reynolds.

I. INTRODUCTION

THE kinematic and dynamic operation of the transmission chain highlights the possible occurrence of vibration. To eliminate these vibrations a tension guide is mounted that tense the branch chain driven either by mounting or using elastic plates or hydraulic systems [1], [2].

This paper presents by finite element analysis the contact between toothed link and tensioning guide. Maximum pressure variation in the contact plates will cause dependence between strength and pitch. At the end of the paper it is highlighted the variation of the lubricant film pressure variation for the contact guide - chain using Reynolds equation.

II. DETERMINATION OF CONTACT PRESSURE USING FINITE ELEMENT METHOD

Generally, for the mechanical systems are frequently the situations when, their elements become instable, because of the constructive shape and connections. A solution to resolve this is to remove the functionality of some mechanical systems elements, which can have serious consequences on the entire mechanichal system. The finite element analysis of these mechanichal structures, assume to identify the displacement and tension fields; this is mainly aimed in determining the displacements, rigidities and equivalent tensions for comparison with the admissible limits, and also to use in subsequent dynamic calculus [3]-[5]. The finite element

analyses of these structures are made successively, begining with structures obtained through clasical calculus and ending through step by step modification with the optimum solution which proposes a minimal mass and maximum rigidity in accepted resistance conditions. For chain and tensioning guide contact, the analysis porpose is to determine the contact pressure, to be used for subsequent analysis on the tribological chain and tensining guide contact [5]-[9].

The virtual model was made using the Catia v5 software, where the main components are modelled as different parts. Then by considering the geometrical constraints between the toothed chain links and the tensioning guide, the final assembled model is obtained.

The virtual model of the toothed chain and tensioning guide system is presented in Fig. 1. In this model, the links are in different contact type with the tensioning guide.
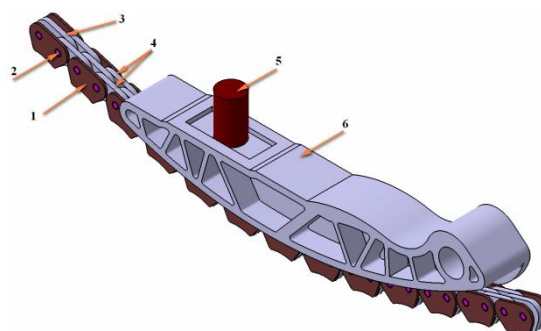

Fig. 1. Toothed chain tensioning:
1- guiding sprockets links; 2- bolts; 3- interior link; 4- exterior link; 5- pressure cylinder; 6- tensioning guide.

For numerical evaluation of the studied model a high performance finite elements computing software Ansys Workbench was used. Given that the contact pressure between the tooth links of the chain and the tensioning guide the materials for these two components are of explicit interest. Basically for the tooth links, bolts and pressure cylinder a steel with the following properties was used [10], [11]:

1) Young's Modulus $E = 200000$ (MPa);
2) Poisson ratio $v = 0.3$;
3) Tensile Yield Strength - TYS $\sigma_{02} = 250$ (MPa);
4) Ultimate Strength - UTS $\sigma_R = 460$ (MPa).

For the guide polyamide PA66 was used with the following properties:
1) Young's Modulus $E = 3300$ (MPa);
2) Poisson ratio $v = 0.42$;
3) Tensile Yield Strength - TYS $\sigma_{02} = 38.8$ (MPa);
4) Ultimate Strength - UTS $\sigma_R = 70$ (MPa).

The constraints application method of the model and the boundary conditions imposed are shown in Fig. 1, where the force, $F = 137$ (N), was applied normal to the surface of the pressing element, the chain was fastened at the ends for all degrees of freedom and for the guide tensioning five degrees of freedom were restricted, allowing one translation. How the transmission from the point of application of force to the chain is only done through contacts between components, also in Fig. 2, are shown also the contact areas defined in Ansys.
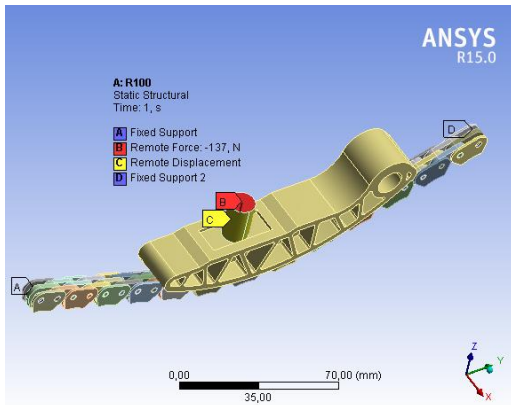

Fig. 2. The finite element model

The model was discretized with finite elements of solid deformable hexahedron and second order node tetrahedron integration. The model discretization result is shown in Fig. 3.
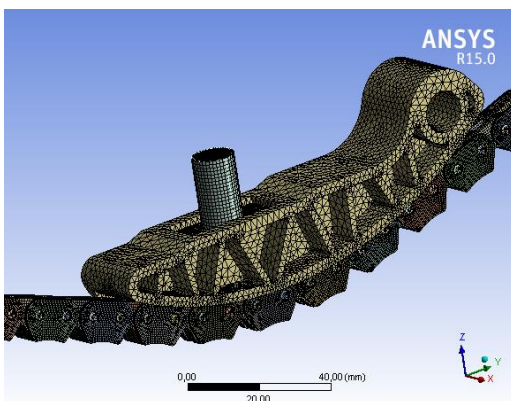

Fig. 3. Meshing model

Due to the force applied to obtain a uniform displacement theoretical distribution with a maximum displacement resulting from 0.038 (mm). This is shown in Fig. 4.
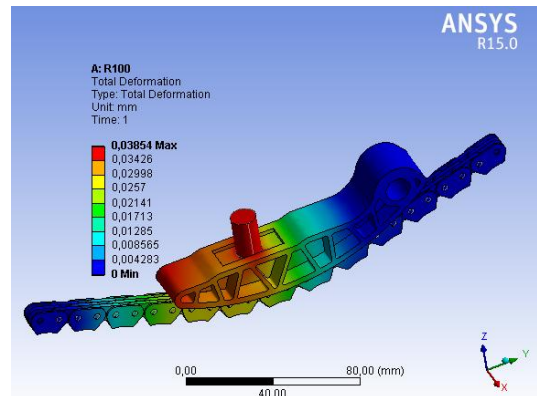

Fig. 4. Displacement distribution

In Fig. 5, is shown the Von Mises stress distribution. It shows that the maximum stresses appear on the links, $\sigma = 300$ (MPa), with acceptable values. The pressures between links and guide reach a maximum of approximately 23 (MPa), which is also acceptable.
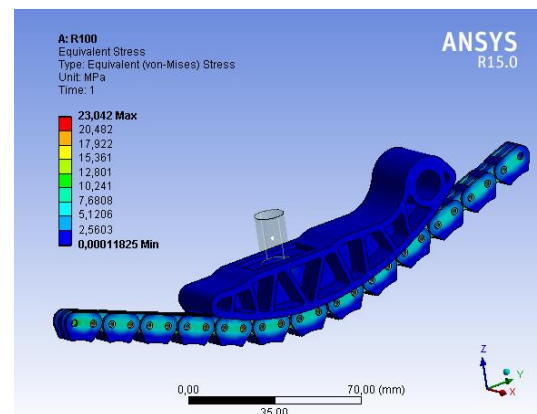

Fig. 5. Von Mises Stress.

The contact between the guide and toothed guide was used friction coefficient of 0.2 and as a result of applied force of 137 (N), we obtained a theoretical distribution of contact pressure, Fig. 6.

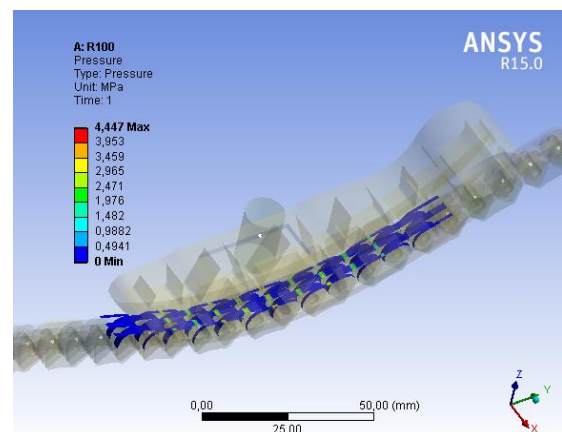The value of maximum contact pressure is 4.44 (Mpa).

Fig. 6. The maximum contact pressure.

Fig. 6 says that the pressure is distributed uniformly on the links due to the position of the chain tensioner area.

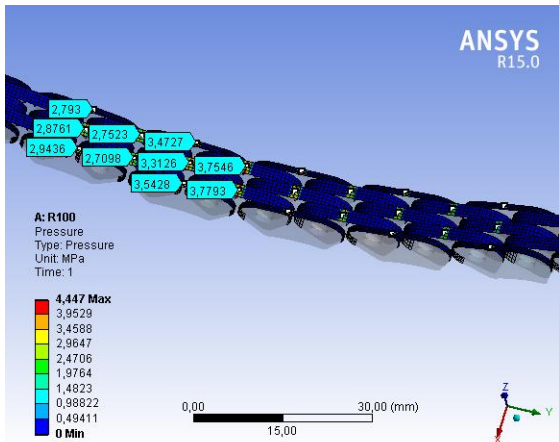To get exactly the links in contact pressure variation, maximum values are read. This is shown in Fig. 7.

Fig. 7. The pressure distribution of the tooth links.

Making an average of the values obtained next paragraph will present in detail the pressure variation for:
guiding sprockets links;
interior links and
exterior links.

Fig. 8 presents the pressure variation of the exterior links depending by the ratio x/p, where:
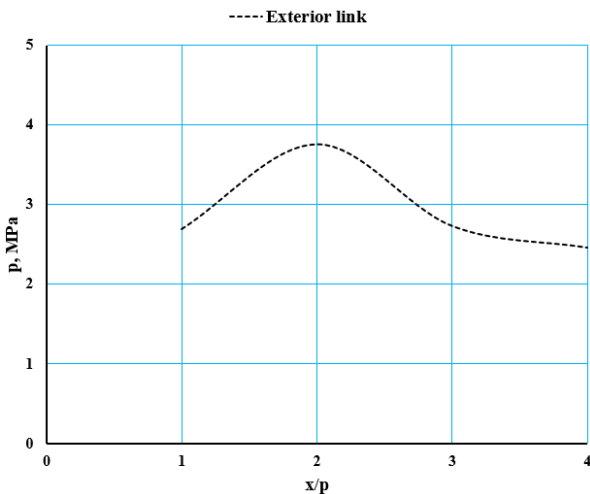p- is the chain pitch, and
x- represent the lenght on the contact.

Fig. 8. The pressure variation of the exterior links

This chart tell us that pressure is the applied force area, then drops to the last links out of contact with guide. In this case was considered as pressure the medium value of the pressure values for the exterior links.

In Fig. 9, is presented the pressure variation of the guiding sprockets link and interior link depending by the ratio x/p.
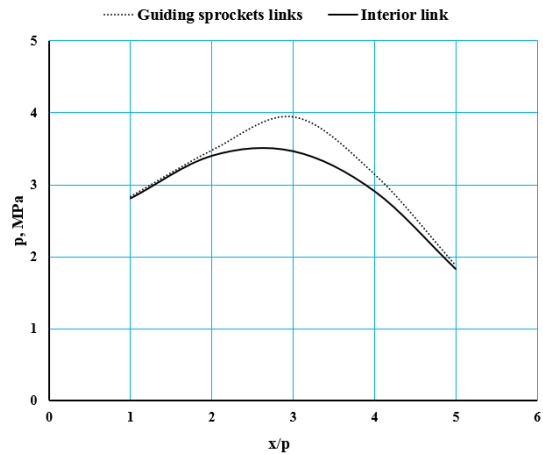

Fig. 9. The pressure variation of the guiding sprockets link and interior link

Previously determined pressures are useful in determining the graphical dependence between F/b ratio versus time.

This dependence is given by relation [12]:

$$\frac{F}{b} = \frac{4 \cdot \pi \cdot R \cdot p_{max}^2}{E_{red}} \; , \qquad (1)$$

where:
b – is the links width (b = 2.19 mm);
F – represent the force links are in contact;
R – is the radius of tensioning guide;
p_{max} – maximum pressure on each links in contact with the guide profile;
E_{red} – reduced Young's modulus for tensioning guide and tooth chain.

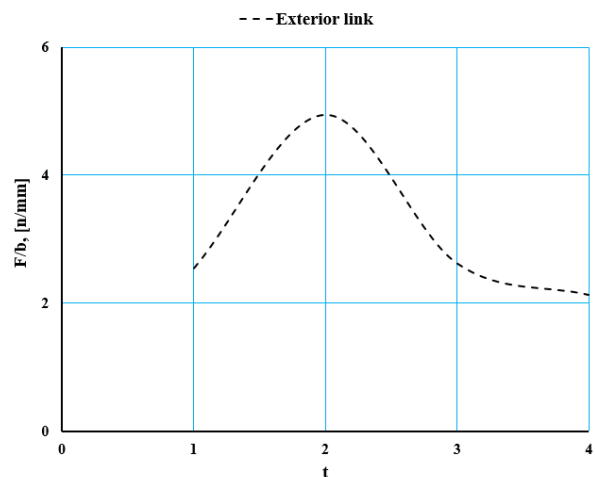Fig. 10 presents the force variation of the exterior links.

Fig. 10. The force variation of the exterior links

Also, Fig. 11, presents the force variation of the guiding sprockets link and interior link.
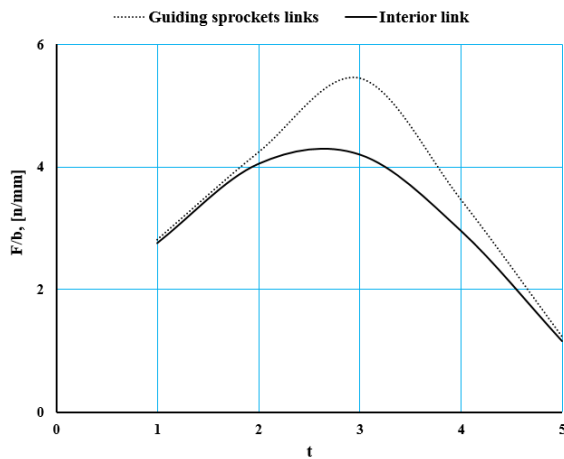
Fig. 11. The force variation of the guiding sprockets link and interior links

Based on diagrams shown in Fig. 10 and Fig. 11, it can be observed that the force depends on the width of the links in contact with guide profile.

III. REYNOLDS EQUATION-ASSUMPTIONS AND SOLVING

For this case of tribological contact for guide − chain contact is the cylinder/cylinder case, was it is presented in Fig. 12. The geometrical and functional parameters of this contact, applied for tensioning guide − chain contact can be also observed. The cylinder 1, with radius R_1, corresponding to the chain link is considered moving with speed U_1 relative to the cylinder 2, the tensioning guide, having the radius R_2, which is considered fixed.
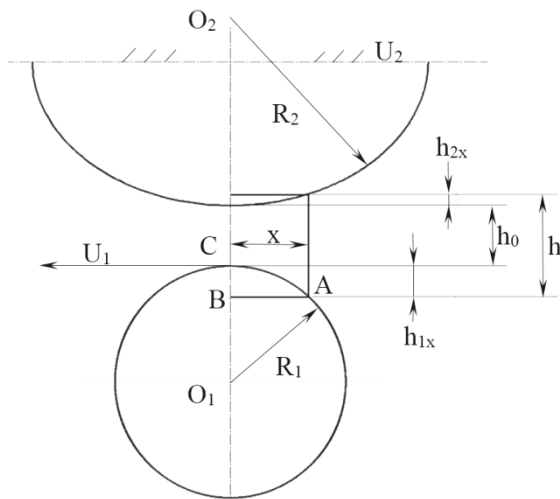

Fig. 12. Guide/chain contact

This relative speed is given by relation

$$U_1 = \frac{\pi}{60} \cdot n_1 \cdot D_{d1} , \tag{2}$$

where n_1 is the rotational speed and D_{d1} the pitch diameter of the driving sprocket.

The one-dimensional Reynolds equation [12]-[14], considering uniform distribution of pressure on the depth of the lubricating film is

$$\frac{dp}{dx} = 12 \cdot \eta \cdot \overline{U} \cdot \frac{h - \overline{h}}{h^3} , \tag{3}$$

where:
η − represents the oil viscosity;
h − represents the lubricant film thickness;
$\overline{h}$ − lubricant film thickness in the point of maximum pressure $x = -\overline{x}((\frac{dp}{dx})_{x=-\overline{x}} = 0)$; Pressure will have a minimum at exiting the narrow space at coordinate $x = -\overline{x} \cdot ((\frac{dp}{dx})_{x=-\overline{x}} = 0)$, where $h = \overline{h}$ [12]-[14];
$\overline{U}$ is the medium speed of the lubrication film

$$\overline{U} = \frac{1}{2} \cdot (U_1 + U_2) = \frac{U_1}{2} . \tag{4}$$

The thickness of the lubricant film, h, at the coordinate x is given by the relation:

$$h = h_0 + h_{1x} + h_{2x} , \tag{5}$$

where:
h_0 − minimum lubricating film thickness
h_{1x}, h_{2x} − lubricant film thickness relative to the coordinate x, can be approximated with following relations:

$$h_{1x} \approx \frac{x^2}{2R_1} \tag{6}$$

and

$$h_{2x} \approx \frac{x^2}{2R_2} . \tag{7}$$

For the reduced curvature:

$$\frac{1}{R} = \frac{1}{R_1} + \frac{1}{R_2} . \tag{8}$$

Applying (6), (7) and (8) in (5) it becomes:

$$h = h_0 + \frac{x^2}{2R} \tag{9}$$

The resulted Reynolds equation is

$$\frac{dp}{dx} = \frac{6 \cdot \eta \cdot U_1}{h_0^2}\left[\frac{1}{\left(1+\dfrac{x^2}{2Rh_0}\right)^2} - \frac{\bar{h}}{h_0\left(1+\dfrac{x^2}{2Rh_0}\right)^3}\right]. \quad (10)$$

The following boundary conditions must be used in order to solve equation (10):

Pressure at exiting the narrow space, is equal to 0, $p(\bar{x}) = 0$;

Pressure at entering the space $p\left(-\dfrac{p}{2}\right) = 0$;

Normal load on the contact is

$$F = l\int_{-\frac{p}{2}}^{\bar{x}} p\,dx, \quad (11)$$

where l is the width of the contact.

Equations (10) and (11) form a system from which the results are: pressure distribution p(x) (coordinate $\bar{x}$) and minimum gap of the space h_0.

IV. REYNOLDS EQUATION - NUMERICAL COMPUTING

The values and also the range of the parameters, used as inputs in determining the pressure distribution for the tensioning guide – toothed chain contact, considering the case of a given real transmission, with variable speeds and constant tensioning, are presented in "TABLE" 1.

TABLE I
PARAMETERS AND VALUE RANGE

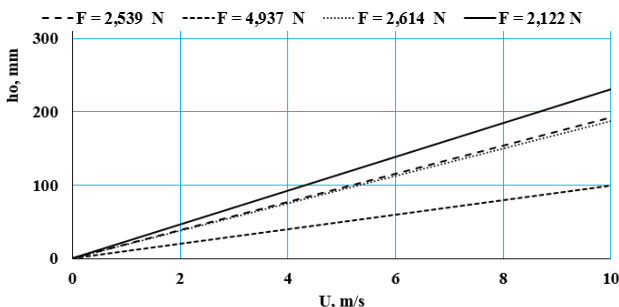| Parameter	Symbol, value (range)
Chain link radius, m	$R_1 = 5\cdot10^{-3}$
Guide radius, m	$R_2 = 0.1$
Reduced curvature, m	$R_r = 0.03$
Dynamic viscosity, Pas	$\eta = 0.150$
Driving sprocket pitch diameter, m	$D_{d1} = 0.05$
Driving sprocket rotational speed, rpm	$n_1 = 500...5000$
Chain speed, m/s	$U_1 = 1...10$
Link normal force, N	$F = 1...6$
Chain link width, m	$l = 2\cdot10^{-3}$

Fig. 13. Minimum gap of the space h_0, depending on relative speed, for exterior links

In Fig. 13, is presented the variation of the minimum gap of the space h_0, depending on relative speed, for given values of forces.
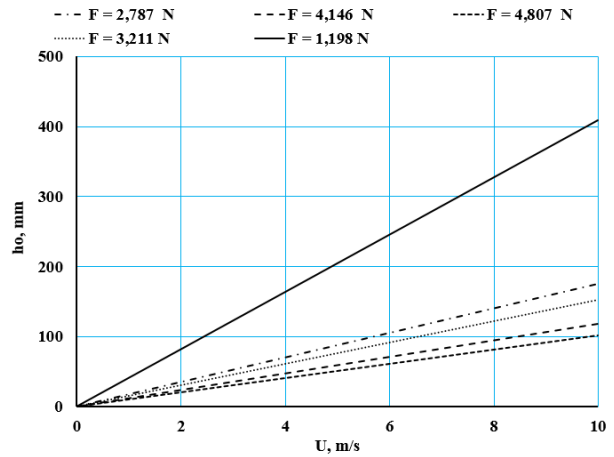

Fig. 14. Minimum gap of the space h_0, depending on relative speed, for guiding sprockets link and interior link

Also, in Fig. 14, is presented the variation of the minimum gap of the space h_0, depending by normal force, for given values of relative speed.
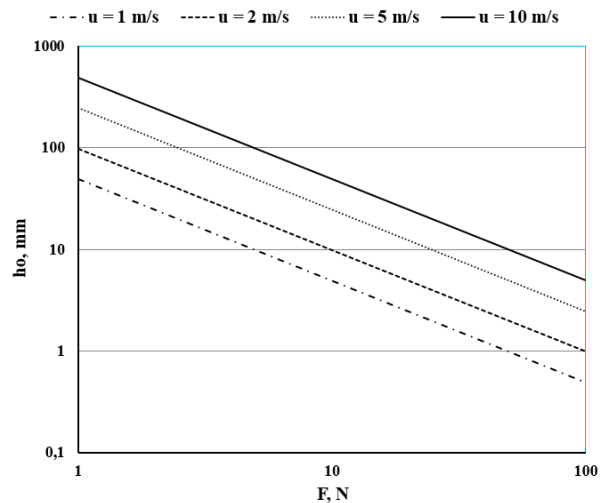

Fig. 15. Minimum gap of the space h_0, depending on normal forces, for few values of relative speed

From the Fig. 14, Fig. 15 and Fig. 16 can be observed that the minimum gap of the space is decreasing below a minimum gap value, considered at least 5 (μm), corresponding to mixed lubrication instead of ideal hydrodynamic lubrication, for smaller vales of speed and higher values of normal force.

In the Fig. 16 and Fig. 17 is presented, for the value of the relative speed U = 5 (m/s), the pressure variation for different values of normal force and narrow space x. As it was presented, the narrow space is depending by the geometry of the contact: the smallest radius of the chain link was considered R = 0.03 (m), straight face of the chain link and maximum radius of the tensioning guide was considered R = 0.1 (m).
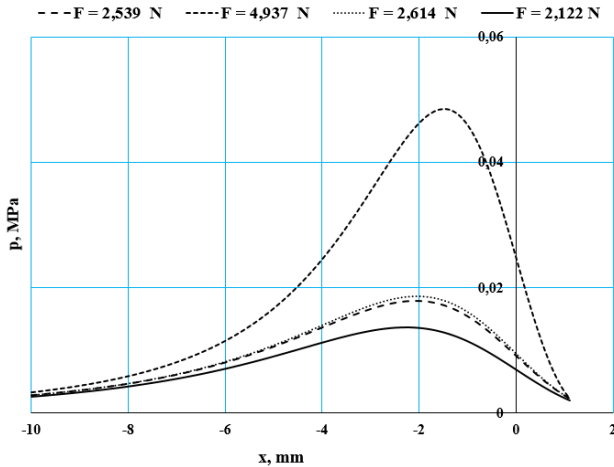
173

Fig. 16. Pressure distribution for relative speed U = 5 (m/s) for exterior link

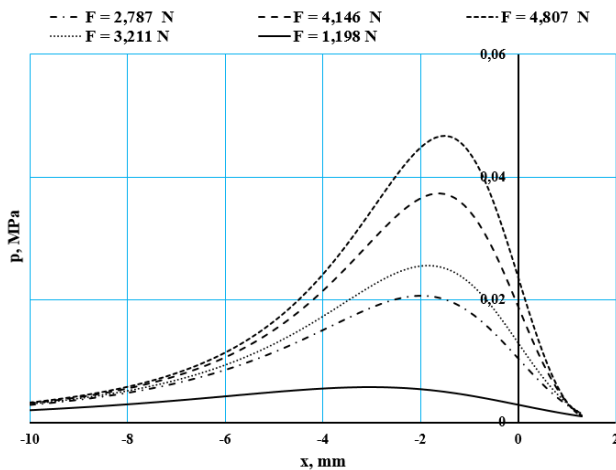

Fig. 17. Pressure distribution for relative speed U = 5 (m/s) for guiding sprockets link and interior link

Fig. 16 and Fig. 17 show the move of the point of maximum pressure towards the minimum gap point (decrease of $\overline{x}$) with increase of normal load.

V. CONCLUSION

The FEM analysis on the virtual model led to contact pressure values between toothed link and tensioning guide. This pressure are use full to obtain the diagrams for the graphical dependence between the toothed chain pitch and x/p ratio, respectively between F/b ratio and time.

Pressure distribution depends on geometry of contact, materials and geometry of the guide, but also on the construction of the chain guide pressing system.

The results of contact pressure between toothed chain link and tensioning guide are considered as inputs for the tribological dynamic analysis in the case of this type of contact.

The results provide useful data in study of the transition between boundary, mixed and hydrodynamic lubrication conditions, applied for the tensioning guide and toothed chain contact used in combustion engines. It also gives the necessary data for optimizing of the toothed chain and tensioning guide geometry.

For more accurate data, an analysis by considering the pressure distribution on the width of the contact should be performed as future research.

Another important purpose of the research is the tensioning guide shape optimization with the goal to reduce the friction and improve the toothed chain transmission durability.

REFERENCES

[1] D. N. Reshetov, *"Machine design,"* Ed. Mir Publisher, Moscow, 1978, pp. 411-436.
[2] H. Roloff, W. Matek, s.a., "Machine elements, Organe de masini," Ed. Matrix Rom, Bucureşti, vol. 2, 2008, pp. 652-668.
[3] X, Wang, L. Hua, *"Analysis of guide modes in vertical hot ring rolling and their effects on the ring's dimensional precision using FE method,"* Springer, pp. 655-662, 2010.
[4] C. Jaliu, R. Velicu, R. Papuc, *"Tensioning and guiding systems used in chain drives,"* Analele Universităţii din Oradea, Fascicula Management şi Inginerie Tehnologică, vol. XXII (XI), Nr.1, Editura Universităţii din Oradea, 2013, pp. 257-260.
[5] R. Papuc, R. Velicu, *"Tribological study of guide-chain contact"* Analele Universităţii din Oradea, Fascicula Management şi Inginerie Tehnologică, vol. XI (XXI), Nr.2, Editura Universităţii din Oradea, 2012, pp. 2.17-2.22
[6] F. Zengming, C. Yabing, Z. Lei, *"Dynamic simulation and analysis of automotive engine's timing silent chain system,"* 5th Asian Conference on Multibody Dynamics, Japan, pp 21-25, 2010.
[7] P.K. Goenka, *"Dynamically Loaded Journal Bearings: Finite Element Method Analysis,"* Trans. ASME Ser. F, Journal of Tribology, vol. 106, pp. 429-439, 1984.
[8] L. L., Kent, *"Structural and thermal analysis using the Ansys Workbench release 14 environment,"* Ed. Stephen Schroff, 2012.
[9] J. Vlasrnik, *"Chain drive computional model as virtual engine module,"* Ph.D. Thesis. Brno University of Technology, Česká Republika, pp. 7-87, 2009.
[10] B. Mouhmid, A. Imad, N. Benseddiq, D. Lecompte, *"An experimental analysis of fracture mechanisms of short glass fibre reinforced polyamide 6,6 (SGFR-PA66)",* Composites Science and Technology, vol. 69, Elsevier, pp. 2521–2526, 2009.
[11] T. Fink, H. Bodenstein, *"Friction Reduction Potentials in Chain Drives,"* MTZ worldwide Edition, Vol.72, pp. 1-8, 2011.
[12] G. W. Stachowiak, A.W. Batchelor, *"Engineering tribology,"* Ed. Elsevier, 3rd ed., Burlington, 2005.
[13] J. Williams, "*Engineering tribology*," Ed. Cambridge University Press, New York, 2011.
[14] W. Shizhu, H. Ping, *"Principles of tribology,"* Ed. Tsinghua University Press, Singapore, 2012.